AIP | Physics of Plasmas

Coupled ion acoustic and drift waves in magnetized superthermal electron-positron-ion plasmas

Muhammad Adnan, S. Mahmood, and Anisa Qamar

Citation: Physics of Plasmas (1994-present) **21**, 092119 (2014); doi: 10.1063/1.4896346
View online: http://dx.doi.org/10.1063/1.4896346
View Table of Contents: http://scitation.aip.org/content/aip/journal/pop/21/9?ver=pdfcov
Published by the AIP Publishing

PHYSICS OF PLASMAS 21, 092119 (2014)

Coupled ion acoustic and drift waves in magnetized superthermal electron-positron-ion plasmas

Muhammad Adnan,[1,2] S. Mahmood,[2,3,4] and Anisa Qamar[1,2]
[1]Institute of Physics and Electronics, University of Peshawar, Peshawar 25000, Pakistan
[2]National Center for Physics, Quaid-i-Azam University Campus, Shahdra Valley Road, Islamabad 44000, Pakistan
[3]Theoretical Physics Division, PINSTECH P.O. Nilore Islamabad 44000, Pakistan
[4]Physics Institute, Federal University of Rio Grande do Sul (UFRGS), 915051-970, Porto Alegre, RS, Brazil

(Received 26 April 2014; accepted 9 September 2014; published online 26 September 2014)

Linear and nonlinear coupled drift-ion acoustic waves are investigated in a nonuniform magnetoplasma having kappa distributed electrons and positrons. In the linear regime, the role of kappa distribution and positron content on the dispersion relation has been highlighted; it is found that strong superthermality (low value of κ) and addition of positrons lowers the phase velocity via decreasing the fundamental scalelengths of the plasmas. In the nonlinear regime, first, coherent nonlinear structure in the form of dipoles and monopoles are obtained and the boundary conditions (boundedness) in the context of superthermality and positron concentrations are discussed. Second, in case of scalar nonlinearity, a Korteweg–de Vries-type equation is obtained, which admit solitary wave solution. It is found that both compressive and rarefactive solitons are formed in the present model. The present work may be useful to understand the low frequency electrostatic modes in inhomogeneous electron positron ion plasmas, which exist in astrophysical plasma situations such as those found in the pulsar magnetosphere.
[http://dx.doi.org/10.1063/1.4896346]

I. INTRODUCTION

Ion acoustic and drift waves are the two fundamental modes of magnetized inhomogeneous plasma in the low frequency limit, i.e., $\omega \ll \Omega_i = \frac{eB_0}{m_i c}$. Ion acoustic waves are basically electrostatic longitudinal perturbations and can propagate in homogeneous unmagnetized plasmas as well through the intermediary of the electric field. On the other hand, drift waves are low frequency electrostatic waves, which propagates in the perpendicular direction to the external magnetic field, i.e., in the y-axis (say) with $k_\perp \gg k_\parallel$, while x-axis being the direction of density gradients and the external magnetic field B_0 is along the z-axis. Drift waves are similar to ion acoustic waves in a way that electrons provide elasticity through the pressure and ions provide the inertia. The main difference between the ion acoustic and drift wave is that energy equipartition between the ion kinetic and potential holds for ion acoustic wave, while for the case of long wavelength drift mode, it does not hold and rather the ion kinetic energy is subdominant; therefore, the potential energy of the ions mainly contribute in the energy density of the system. For large parallel wave vector ($k_\parallel$), drift wave can turn into ion acoustic waves.[1]

Electrostatic waves with Maxwellian particle distribution have been studied since long ago; however, it is well established now by evidence from both space[2–5] and laboratory[6,7] plasmas that non-Maxwellian particle distributions are required to model efficiently the role of energetic particles, associate with long-tailed (superthermal) velocity distributions. Such particles (electrons and positrons in our case) can be modeled by kappa or generalized Lorentzian velocity distribution function, which imply the Maxwellian core and a high energy tail component of the power law form. The form of the kappa distribution was first postulated by Vasyliunas in 1968[2] to fit observational solar wind data. By now, the kappa distribution has been employed to explain many astrophysical and space plasma situations, e.g., in the auroral zone,[8] in the Earth's magnetosphere,[9] in the interstellar medium,[10] and the solar wind.[11] Interestingly, non-Maxwellian energetic particles are also observed in the lab.[6,7] The three dimensional isotropic kappa velocity distribution function for superthermal particles can be written as[2]

$$f_\kappa(v) = \frac{n_{j0}}{(\pi\kappa\theta^2)^{3/2}}\frac{\Gamma(\kappa+1)}{\Gamma(\kappa-1/2)}\left(1+\frac{v^2}{\kappa\theta^2}\right),$$

where $\theta = \{(\kappa-3/2)/\kappa\}^{1/2}(2k_BT_e/m_e)^{1/2}$ represent the effective or modified speed of the superthermal particles having thermal speed or the most probable speed in Maxwellian plasmas as $v_{te} = (2k_BT_e/m_e)^{1/2}$. The spectral index κ measures the slope of the energy spectrum of the superthermal particles at the tail of the distribution function such that smaller (larger) values of κ represent high (low) concentrations of superthermal particles in the tail of the distribution function and $\kappa > 3/2$ should hold for a physically valid solution. Other parameters include $\Gamma(x)$, which represent gamma function and n_{j0} is the equilibrium density of the jth species. In the limit of $\kappa \to \infty$, the above distribution function reduces to Maxwellian limit.

The drift waves were theoretically predicted by Rudakov and Sagdeev,[12] while experimentally verified by D'Angelo and Motley[13] decades ago. It is well established now that magnetized plasma system contains regions of inhomogeneity, which can cause a variety of drift oscillations. The interest in these modes is due to their importance in the anomalous transport of a plasma in the perpendicular direction to a magnetic field. Low frequency coupled ion acoustic and drift waves are fundamental linear modes of inhomogeneous magnetized plasmas. However, the nonlinearities present in the system can give rise to coherent nonlinear structures such as solitons, vortices, shocks, etc. Structures associated with drift waves can only exist in magnetized plasmas having inhomogeneity (e.g., in density, temperature, magnetic field, etc.), while acoustic type nonlinear structures can be present both in magnetized and unmagnetized homogenous plasmas.[14]

Mirza *et al.*[15] studied low frequency electrostatic waves in a magnetized plasma in the presence of sheared flow. They showed that, for specific profiles of the equilibrium shear flow, the linear equations admit a tripolar vortex solution; similarly, electromagnetic vortices have been reported in electron positron ion plasmas in the Ref. 16. Mushtaq *et al.*[17] reported the linear and nonlinear coupled drift and ion acoustic waves with Maxwellian electrons in a collisional magnetoplasma. Masood and Ahmad investigated the linear modes of coupled dispersive drift acoustic modes in nonuniform plasmas in the presence of nonthermal particle distributions[18] while Shan and Haque[19] traced out nonlinear dipolar and monopolar vortex solutions in the presence of superthermal electrons. Recently, Mahmood *et al.*[20] studied electrostatic vortex structures in a multicomponent plasma. They discussed dispersion relation in both localized and nonlocalized limits and found the condition for the existence of dipolar vortex structures in a magnetized rotating electron-positron plasma with stationary ions.

Electron positron ion (e-p-i) plasmas have been extensively studied in the recent years[21–26] due to their existence in the astrophysical environments, example includes, magnetosphere of neutron stars,[27] in active galactic cores,[28] and in solar flare plasma.[29] Importantly, these three component plasmas have also been produced in the laboratory,[30–32] and the existence of positrons in other laboratory plasmas has been confirmed.[33–35] The process of pair production (electron–positron) can occur during the interaction of a strong laser pulse with plasmas,[36–39] as well as by the interaction of superthermal electrons with high-Z material.[40] The production of positrons in the laboratory having energies in the mega electron volts has lead to more antimatter research, including the investigation of the physics underlying various astrophysical phenomena such as gamma ray bursts, positronium production, and Bose-Einstein condensates.[41,42] The properties of the conventional electron-ion plasma changes due to the presence of positrons, as it reduces the ion number density in the system. On the same time scale, the dynamics of electrons and positrons could be the same, the two having the same mass (but different charge). Therefore, kappa distribution can be assumed for physical environments having excess superthermal (high-energy) charged particles. Importantly, the interaction of high energy gamma ray photons with the atoms/molecules leads to the generation of high energy electrons and positrons in the interstellar medium[43] and earth upper atmosphere.[44–47] Similarly, the plasma sheet boundary of earth magneto-tail also contains such energetic particles (nonthermal) originating partially from the pulsar into the low density interstellar plasma.[48–50]

In this manuscript, we have analyzed linear and nonlinear waves in a magnetized e-p-i plasma having inertial cold ions, kappa distributed electrons, and positrons. In the linear regime, we emphasized on the effects of kappa distribution and positron content on the phase velocity of the coupled drift ion acoustic waves in the presence of density inhomogeneity and discussed various possible limits of the dispersion relation. In the nonlinear regime, first, we obtained stationary solutions in the form of a dipolar and monopolar vortices, highlighting the role of kappa distribution and plasma configurations on the formation of vortices solutions. Second, in the case of weak dispersion (low frequency perturbations) and scalar nonlinearity, we presented the formation of drift solitary waves and discussed the importance of spectral index (κ) on the solitary structures in an inhomogeneous magnetized plasma.

II. BASIC MODEL EQUATIONS

We consider an inhomogeneous, three component magnetoplasma consisting of inertial cold ions, kappa distributed electrons, and positron. The external magnetic field is uniform and taken along the $\hat{z}$-axis, i.e., $\vec{B} = B_0\hat{z}$. The plasma number densities have gradients in their equilibrium values along the negative $\hat{x}$-axis and is given by $-dn_{j0}/dx$. The dynamics of drift ion acoustic waves in a magnetoplasma can be described by the following sets of equations:

$$\partial_t n_i + \vec{\nabla}\cdot(n_i\vec{v}_i) = 0, \tag{1}$$

$$\partial_t\vec{v}_i + (\vec{v}_i\cdot\vec{\nabla})\vec{v}_i = -\frac{e}{m_i}\vec{E} - \frac{e}{m_i c}(\vec{v}_i\times B_0\hat{z}), \tag{2}$$

$$n_e = n_{e0}\left[1 - \frac{e\phi}{T_e(\kappa_e - 3/2)}\right]^{-\kappa_e+1/2}, \tag{3}$$

and

$$n_p = n_{p0}\left[1 + \frac{e\phi}{T_p(\kappa_p - 3/2)}\right]^{-\kappa_p+1/2}. \tag{4}$$

To get the expression for the ion perpendicular velocity under low frequency limit, i.e., $|\frac{d}{dt}| \ll \Omega_i$, by taking the vector product of Eq. (2) with $\hat{z}$, we have

$$\vec{v}_{i\perp} = \frac{c}{B_0}\mathbf{E}\times\hat{\mathbf{z}} + \frac{m_i c}{B_0 e}\frac{d}{dt}(\hat{\mathbf{z}}\times\vec{\mathbf{v}}_i) = \vec{v}_E + \vec{v}_p,$$

where $\frac{d}{dt} = (\partial_t + \vec{v}_i.\vec{\nabla})$ and $\frac{d}{dt}(\hat{z}\times\vec{v}_i)$ means $\frac{d}{dt}(\hat{z}\times\vec{v}_{i_\perp})$ and $\hat{z}\times\vec{v}_{i_z} = 0$.

Here, the first term $\vec{v}_E = \frac{c}{B_0}E\times\hat{z}$ represent the $E\times B$ drift, whereas the second term $\vec{v}_p = \frac{m_i c}{B_0 e}\frac{d}{dt}(\hat{z}\times\vec{v}_i)$ is the polarization drift containing the perturbed velocity.

The assumption that $\vec{v}_E \gg \vec{v}_p$ being consistent with our assumption $|\frac{d}{dt}| \ll \Omega_i$ in the drift approximations and can give us the following:

$$\vec{\mathbf{v}}_{i\perp} = \frac{c}{B_0}\vec{\mathbf{E}}\times\hat{\mathbf{z}} + \frac{m_i c}{B_0 e}\frac{d}{dt}(\hat{\mathbf{z}}\times\vec{\mathbf{v}}_E),$$

$$\vec{\mathbf{v}}_{i\perp} = \frac{c}{B_0}\vec{\mathbf{E}}\times\hat{\mathbf{z}} + \frac{m_i c}{B_0 e}\frac{c}{B_0}\frac{d}{dt}\left(\hat{\mathbf{z}}\times(\vec{\mathbf{E}}\times\hat{\mathbf{z}}\right),$$

$$\vec{\mathbf{v}}_{i\perp} = \frac{c}{B_0}\vec{\mathbf{E}}\times\hat{\mathbf{z}} + \frac{c}{B_0\Omega_i}\frac{d}{dt}\left(\vec{\mathbf{E}} - \mathbf{E}_z\hat{\mathbf{z}}\right),$$

$$\vec{v}_{i\perp} = \frac{c}{B_0}\vec{\mathbf{E}}\times B_0\hat{\mathbf{z}} + \frac{c}{\Omega_i}\frac{d}{dt}(\mathbf{E}_\perp),$$

where $\Omega_i = \frac{eB_0}{m_i c}$ and $E_\perp = \vec{E} - E_z\hat{z}$, so

$$\vec{\mathbf{v}}_{i\perp} = \frac{c}{B_0}\vec{\mathbf{E}}\times\hat{\mathbf{z}} + \frac{c}{B_0\Omega_i}\frac{d}{dt}\mathbf{E}_\perp,$$

$$\vec{v}_{i\perp} = \frac{c}{B_0}\hat{z}\times\vec{\nabla}_\perp\phi - \frac{c}{B_0\Omega_i}\frac{d}{dt}\vec{\nabla}_\perp\phi,$$

where $\frac{d}{dt} = (\partial_t + \vec{v}_i.\vec{\nabla}) = \left(\partial_t + \vec{v}_{i\perp}\cdot\vec{\nabla}_\perp + v_z\partial_z\right)$ and under low frequency limit, $|\frac{d}{dt}| \ll \Omega_i$, i.e., $\vec{v}_E \gg \vec{v}_p$, one can obtain the following result:

$$\vec{v}_{i\perp} = \frac{c}{B_0}\hat{z}\times\vec{\nabla}_\perp\phi - \frac{c}{B_0\Omega_i}\left(\partial_t + \vec{v}_E\cdot\vec{\nabla}_\perp + v_z\partial_z\right)\vec{\nabla}_\perp\phi. \tag{5}$$

The ion gyro-frequency is defined as $\Omega_i = \frac{eB_0}{m_i c}$, while ϕ denotes the electrostatic potential defined in the current model. Here, for simplicity, we analyze the plasma dynamics in two-dimension (2D), since only two direction are of relevance, say $\{\|,\perp\} = \{z, y\}$, viz. $\nabla = (0, \partial_y, \partial_z)$. In other words, excitations are assumed to evolve and propagate in the yz -plane, with no loss of generality. Then, ion continuity equation takes the form

$$\partial_t n_i + \vec{\nabla}_\perp\cdot(n_i\vec{v}_{i_\perp}) + \partial_z(n_i v_{iz}) = 0. \tag{6}$$

Assuming small deviations from the equilibrium state, i.e., $\Phi = \left(\frac{e\phi}{T_e}\right) \ll 1$, the superthermal particle densities can be expressed as

$$n_e \simeq \delta\{1 + c_1\Phi + c_2\Phi^2 + \mathcal{O}(\Phi^3)\}, \tag{7}$$

and

$$n_p \simeq p\{1 - d_1\Phi + d_2\Phi^2 + \mathcal{O}(\Phi^3)\}, \tag{8}$$

with expansion parameters c_1, c_2, d_1, and d_2 are functions of the κ, given below

$$c_1 = \left(\frac{\kappa_e - 1/2}{\kappa_e - 3/2}\right), \quad c_2 = \frac{c_1}{2}\left(\frac{\kappa_e + 1/2}{\kappa_e - 3/2}\right),$$
$$d_1 = \sigma\left(\frac{\kappa_p - 1/2}{\kappa_p - 3/2}\right), \quad d_2 = \frac{\sigma d_1}{2}\left(\frac{\kappa_p + 1/2}{\kappa_p - 3/2}\right). \tag{9}$$

The system is closed with plasma approximation or neutrality hypothesis

$$n_i + n_p \sim n_e. \tag{10}$$

Charge balance at equilibrium requires $n_{i0} + n_{p0} = n_{e0}$ $\Rightarrow \delta = 1 + p$, with $\delta = n_{e0}/n_{i0}$ and $p = n_{e0}/n_{i0}$ are defined. Using Eqs. (5) and (10) in ion continuity Eq. (6), one can obtained the following equation:

$$\frac{d}{dt}\left[(\delta c_1 + pd_1)\Phi + (\delta c_2 - pd_2)\Phi^2\right] + v_*\frac{\partial\Phi}{\partial y}$$
$$-\rho_s^2\frac{d}{dt}\nabla_\perp^2\Phi + \frac{\partial v_{iz}}{\partial z} = 0, \tag{11}$$

where $\frac{d}{dt} = \partial_t + \vec{v}_E\cdot\vec{\nabla}_\perp + v_z\partial_z$, $v_* = \frac{cT_e}{eB_0}|\kappa_n|$. $\rho_s^2 = \frac{c_s^2}{\Omega_i^2}$, $\Phi = \left(\frac{e\phi}{T_e}\right)$, $\kappa_n = -\frac{1}{n_{0i}}\frac{\partial n_{0i}}{\partial x}$, and $c_s = \left(\frac{T_e}{m_i}\right)^{1/2}$ have been defined. The parallel component of the ion momentum equation can be expressed in normalized form as

$$\left(\partial_t + \vec{v}_E\cdot\vec{\nabla}_\perp + v_z\partial_z\right)v_{iz} = -c_s^2\frac{\partial\Phi}{\partial z}. \tag{12}$$

III. LINEAR ANALYSIS

The linear dispersion relation (DR) is obtained by assuming small perturbations $\sim e^{i(k_y y + k_z z - \omega t)}$, i.e., Fourier analyzing Eqs. (11) and (12) and can be written as

$$\left(1 + \frac{\rho_s^2}{\delta c_1 + pd_1}k_y^2\right)\omega^2 - \frac{\omega_*}{\delta c_1 + pd_1}\omega - \frac{c_s^2}{\delta c_1 + pd_1}k_z^2 = 0. \tag{13}$$

The structure of the DR is self-explanatory: one can see the effect of superthermality through c_1, d_1 (recovering a Maxwellian limit for $\kappa_{e,p}\to\infty$) and positron content through p; further to this, it is evident from the above DR, that the gyroradius $\rho_s = \frac{c_s}{\Omega_i}$, the frequency of the drift waves, $\omega_* = v_* k_y$, and the ion sound speed $c_s = \left(\frac{T_e}{m_i}\right)^{1/2}$ have been modified. One can re-write Eq. (13) in the following form:

$$(1 + \rho_{s\kappa}^2 k_y^2)\omega^2 - \omega_{*\kappa}\omega - c_{s\kappa}^2 k_z^2 = 0, \tag{14}$$

with

$$\rho_{s\kappa} = \frac{\rho_s}{\sqrt{\delta c_1 + pd_1}},$$
$$\omega_{*\kappa} = \frac{\omega_*}{\delta c_1 + pd_1}, \text{ and} \tag{15}$$
$$\mathbf{c}_{s\kappa} = \frac{c_s}{\sqrt{\delta c_1 + pd_1}}.$$

Equation (15) essentially reflect that superthermality and positron content tighten up the gyroradius, reduces the frequency of the drift waves and ion sound speed with respect to a Maxwellian limit for $\kappa_{e,p}\to\infty$.

For pure acoustic mode, i.e., $k_y = 0$, one can reduce Eq. (14) to the following limit in superthermal e-p-i plasma:

$$\omega = c_{s\kappa}k_z. \tag{16}$$

While on the other hand, for pure drift waves, i.e., $k_z = 0$, Eq. (14) takes the following form:

$$\omega = \frac{\omega_{*\kappa}}{\left(1 + \rho_{s\kappa}^2 k_y^2\right)}. \tag{17}$$

The dispersion relation obtained here can be reduced to the work of Ref. 19 based on superthermal electron-ion plasma by setting $p = 0$ and $\delta = 1$; similarly, for

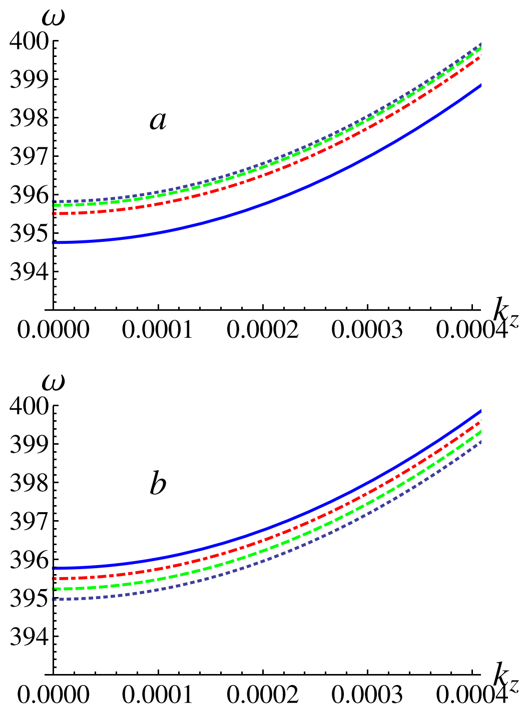

FIG. 1. Frequency of coupled drift ion acoustic waves is plotted against k_z for different values of superthermality parameter and positron content. Plot (a): ω versus k_z with $p = 0.2$ for $\kappa_e = \kappa_p = 2$ (solid blue curve), $\kappa_e = \kappa_p = 3$ (dotted–dashed red curve), $\kappa_e = \kappa_p = 5$ (dashed green curve), and $\kappa_e = \kappa_p = 10$ (dotted blue curve). Plot (b): ω versus k_z with $\kappa_e = \kappa_p = 3$ for $p = 0$ (solid blue curve), $p = 0.2$ (dotted–dashed red curve), $p = 0.4$ (dashed green curve), and $p = 0.6$ (dotted blue curve). The values of other parameters are $k_y = 0.02$ and $\kappa_n = k_y/5$.

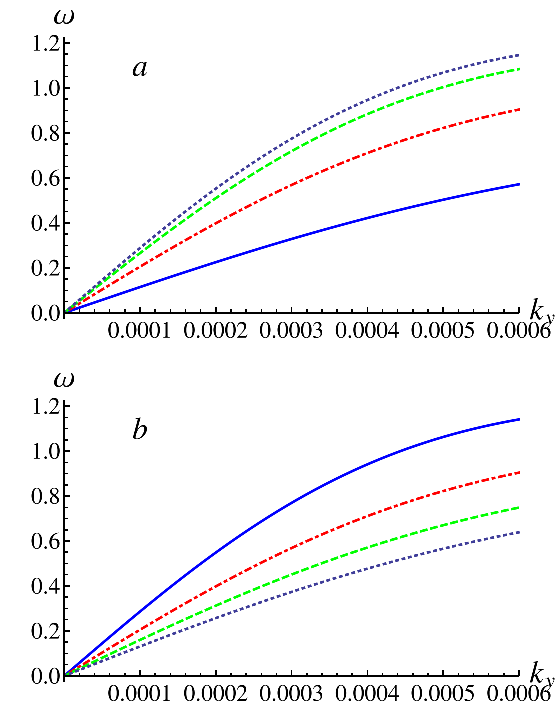

FIG. 2. Frequency of coupled drift ion acoustic waves is plotted against k_y for different values of superthermality parameter and positron content. Plot (a): ω versus k_y with $p = 0.2$ for $\kappa_e = \kappa_p = 2$ (solid blue curve), $\kappa_e = \kappa_p = 3$ (dotted–dashed red curve), $\kappa_e = \kappa_p = 5$ (dashed green curve), and $\kappa_e = \kappa_p = 7$ (dotted blue curve). Plot (b): ω versus k_y with $\kappa_e = \kappa_p = 3$ for $p = 0$ (solid blue curve), $p = 0.2$ (dotted–dashed red curve), $p = 0.4$ (dashed green curve), and $p = 0.6$ (dotted blue curve). The values of other parameters are $k_z = 10^{-10}$ and $\kappa_n = 10^{-6}$.

Maxwellian electron-ion plasma case, one can recover the textbook limit[1] by taking $\kappa_{e,p} \to \infty$ in our dispersion relation. The work of Haque and Saleem[51] on electron positron ion plasma with Maxwellian distribution can also be deduced from Eq. 14 by putting $\kappa_{e,p} \to \infty$.

In Figure 1, we have shown the effect of superthermality and positron content on the frequency of drift ion acoustic waves based on Eq. (14). In Figure 1(a), one can see that for a fixed value of k_y, increasing the value of κ makes the frequency of the drift ion acoustic waves to escalate, while on the other hand, increasing positron content in the system makes the frequency to suppress. Here, it is important to mention the following realities: (i) the frequency of pure drift waves (at $k_z = 0$) in Figure 1 decreases with strong superthermality (low value of κ) as well as with positron content through increasing p. (ii) The effect of finite larmor radius is visible on the curves shown in Figure 1. The above two statements are in agreements with Eq. (15). Similarly, in Figure 2, we have plotted the dispersion relation (14) against k_y for a fixed value of k_z (very small but nonzero) such that $k_y > k_z$. One can see in Figure 2, the effect of kappa distribution and positrons on the dispersion relation when the effect of drift waves is dominant over the acoustic waves in our present model.

IV. NONLINEAR VORTICAL STRUCTURES IN SUPERTHERMAL PLASMA

In this section, we anticipate the formation of coherent nonlinear structure in the form of vortices, for this, we adopt the standard procedure. We assume a co-moving frame of reference (x, η) with constant velocity u such that $\eta = y + \alpha z - ut$, where α $(0 < \alpha < 1)$ is the wave coupling parameter. The parallel component of ion momentum Eq. (12) can be written in the new transformed frame with the assumption, $\vec{v}_E \cdot \vec{\nabla}_\perp \gg v_z \partial_z$[1]

$$\frac{d}{dt} v_{iz} = \alpha c_s^2 \left(\frac{\partial}{\partial \eta} + \frac{cT_e}{ueB_0} (\partial_\eta \Phi \partial_x - \partial_x \Phi \partial_\eta) \right) \Phi, \tag{18}$$

where $\frac{d}{dt} = uD_\phi$ with $D_\phi = \left(\frac{\partial}{\partial \eta} + \frac{cT_e}{ueB_0} (\partial_\eta \Phi \partial_x - \partial_x \Phi \partial_\eta) \right)$.

Similarly, one can write the Eq. (11) in the transformed coordinate with the following approximations: In the polarization drift, we assumed $\vec{v}_E \cdot \vec{\nabla}_\perp \gg v_z \partial_z$ and taking only first order term in the plasma neutrality hypothesis, i.e., $\frac{n_{i1}}{n_{i0}} \approx (\delta c_1 + p d_1)\Phi$.

$$\frac{d}{dt} \left[\nabla_\perp^2 - (\delta c_1 + p d_1) \right] \Phi + v_* \frac{\partial \Phi}{\partial \eta} + \frac{\partial v_{iz}}{\partial \eta} = 0. \tag{19}$$

Here, it is important to elaborate the structure of Eq. (19) based on our plasma model: The first term in Eq. (19) arises due to the ion polarization drift, the second term represent the plasma configurations, while the third and fourth are the density gradient and ion parallel motion terms, respectively. In Eq. (19), ∇ has been normalized with ion gyroradius ρ_s, eliminating v_{iz} with the help of Eq. (18), one can write it as

$$D_\phi [\nabla_\perp^2 \Phi - A^2 \Phi] = 0. \tag{20}$$

Equation (20) is a modified Hasegawa-Mima (HM) equation with $A^2 = \delta c_1 + pd_1 - \frac{v_*}{u} - \frac{\alpha^2 c_s^2}{u^2}$. One can see the explicit dependence of $\kappa_{e,p}$ through c_1 and d_1 and effect of positron content appear through the density ratio p. In order to construct Eq. (20), the role of ion polarization drift is mandatory, while A^2 always contains the plasma configurational terms.

In order to find the solution of Eq. (20), we assume a solution of the form

$$\nabla_\perp^2 \Phi - A^2\Phi = f\left(\Phi - \frac{ueB_0}{cT_e}x\right), \quad (21)$$

where $f(\Phi, x)$ is an arbitrary function and under linear approximation can take the form

$$\nabla_\perp^2 \Phi - A^2\Phi = C_1\left(\Phi - \frac{u\Omega_i}{c_s^2}x\right), \quad (22)$$

with C_1 represent some constant. In polar coordinate system, we have position vector $r = (x^2+\eta^2)^{1/2}$ and $\beta = \tan^{-1}\left(\frac{\eta}{x}\right)$; therefore, it is important to divide the plane (r, β) into an outer region $r > r_0$ and inner region $r < r_0$ of a circle of radius r_0, such that the two solutions of Eq. (22) in the above mentioned regions should agree at $r = r_0$.

For outer region, Eq. (22) can be solved with a separation of variable technique, with $C_1 = 0$ as $r \to \infty$ and can be represented as

$$\Phi_{out}(r, \beta) = Q_1 K_1(Ar)\cos\beta, \quad (23)$$

where Q_1 is the integration constant and can be determined with the help of boundary conditions and K_1 is the modified Bessel function of first order and second kind. For physical justification of the above localized solution, it is important that A should be greater than zero for large r ($A > 0$ at $r \to \infty$), as $K_1 \sim \left(\frac{1}{r}\right)^{1/2}\exp(-Ar)$. It is evident from Eq. (23) that argument of Bessel function contains A, and hence, the effect of kappa and positron along with the acoustic and drift speed will affect the characteristics of vortex. For the sake of reference, it is important to mention that our results (see Sec. IV) are in complete agreement with the work of Shan and Haque[19] in the limit of electron-ion plasma.

Similarly, for the inner region $r < r_0$, Eq. (22) gives the solution as

$$\Phi_{in}(r, \beta) = \left[Q_2 J_1(\chi r) + \left(\frac{\chi^2 + A^2}{\chi^2}\right)\frac{c_s^2}{u\Omega_i}r\right]\cos\beta, \quad (24)$$

where Q_2 is constant of integration and $\chi = -(A^2 + C_1)$ is the argument of ordinary Bessel function of first order J_1.

For monopolar solution, one can solve Eq. (22) in the limit of $C_1 = 0$ and the electrostatic potential Φ is only dependent on r,.The result can be expressed as

$$\Phi_{mp}(r) = Q_3 J_0(Ar), \quad (25)$$

where Q_3 is the integration constant and J_0 is the Bessel function of zeroth order. The constant of integrations Q_1, Q_2, and Q_3 along with χ can be determined from the continuity of electrostatic potential Φ across the boundary, i.e., Φ, $\partial_r\Phi$ and $\nabla_\perp^2\Phi$ should be same at $r = r_0$ and can be expressed as

$$Q_1 = \frac{c_s^2}{u\Omega_i}\frac{r_0}{K_1(Ar_0)}, \quad Q_2 = \frac{c_s^2}{u\Omega_i}\left(-\frac{A^2}{\chi^2}\right)\frac{r_0}{J_1(\chi r_0)},$$
$$\frac{K_2(Ar_0)}{K_1(Ar_0)} = -\left(\frac{A}{\chi}\right)\frac{J_2(\chi r_0)}{J_1(\chi r_0)}.$$

V. DRIFT SOLITON IN SUPERTHERMAL PLASMA

In this section, we present the analysis of drift solitary waves in the presence of superthermal electron and positron. For low frequency electrostatic excitations with scalar nonlinearity and weak dispersion, one can assume $\vec{v}_E \cdot \vec{\nabla}_\perp \ll v_z\partial_z$ (Ref. 17) in the polarization drift, which reduce the ion parallel component of momentum Eq. (12) to

$$(\partial_t + v_z\partial_z)v_{iz} = -c_s^2\frac{\partial\Phi}{\partial z}. \quad (26)$$

After transforming Eq. (26) into the co-moving frame, $\eta = y + \alpha z - ut$ and solving for v_{iz}, one can obtain the following expression:

$$v_{iz} = \frac{c_s^2\alpha}{u}\Phi + \frac{c_s^4\alpha^3}{2u^3}\Phi^2. \quad (27)$$

Using the above equation in Eq. (11) after transformation, one can obtain

$$\left[-u\frac{\partial}{\partial\eta} + \left(\frac{c_s^2\alpha}{u}\Phi + \frac{c_s^4\alpha^3}{2u^3}\Phi^2\right)\alpha\frac{\partial}{\partial\eta}\right]$$
$$\times\left[(\delta c_1 + pd_1)\Phi + (\delta c_2 - pd_2)\Phi^2\right] + v_*\frac{\partial\Phi}{\partial\eta}$$
$$-\rho_s^2\left[-u\frac{\partial}{\partial\eta} + \left(\frac{c_s^2\alpha}{u}\Phi + \frac{c_s^4\alpha^3}{2u^3}\Phi^2\right)\alpha\frac{\partial}{\partial\eta}\right]\frac{\partial^2}{\partial\eta^2}\Phi$$
$$+\frac{\partial}{\partial\eta}\left(\frac{c_s^2\alpha}{u}\Phi + \frac{c_s^4\alpha^3}{2u^3}\Phi^2\right) = 0. \quad (28)$$

After a short manipulation, one can obtain the following nonlinear equation:

$$-\left[-(\delta c_1 + pd_1) + \frac{v_*}{u} + \alpha^2\left(\frac{c_s}{u}\right)^2\right]\frac{d\Phi}{d\eta}$$
$$+\left[(\delta c_2 - pd_2) - \frac{\alpha^2}{2}(\delta c_1 + pd_1)\left(\frac{c_s}{u}\right)^2 - \frac{\alpha^4}{2}\left(\frac{c_s}{u}\right)^4\right]\Phi\frac{d\Phi}{d\eta}$$
$$-\frac{d^3\Phi}{d\eta^3} = 0, \quad (29)$$

which represent a KdV type equation for ion acoustic waves coupled with drift waves in a superthermal e-p-i plasmas, yielding solitary wave solution given as

$$\Phi = \left(\frac{3}{A}\right)\sec h^2\left(\frac{\eta}{\rho_s}\sqrt{4B}\right), \quad (30)$$

where $A = A_2/A_1$ and $B = A_3/A_1$ with $A_1 = -[-(\delta c_1 + pd_1) + \frac{v_*}{u} + \alpha^2(\frac{c_s}{u})^2]$, $A_2 = [(\delta c_2 - pd_2) - \frac{\alpha^2}{2}(\delta c_1 + pd_1)(\frac{c_s}{u})^2 - \frac{\alpha^4}{2}(\frac{c_s}{u})^4]$, and $A_3 = -1$. For physically valid solution $B > 0$, i.e., $[(\delta c_1 + pd_1) - \frac{v_*}{u} - \alpha^2(\frac{c_s}{u})^2] > 0$. The solitary waves described in Eq. (30) may give either positive (compressive) or negative (rarefactive) pulse, depending on the sign of the nonlinearity coefficient A. One can see the role of kappa distribution through c_1, d_1, and the role of positrons appears through p in the above coefficients. In Figure (3), we have shown the effect of superthermality parameter (κ), wave coupling constant (α) and positrons content (p) on the nonlinearity coefficient A and hence the amplitude (ϕ_m) of the solitary waves, as the two are related by $\phi_m = \frac{3}{A}$.

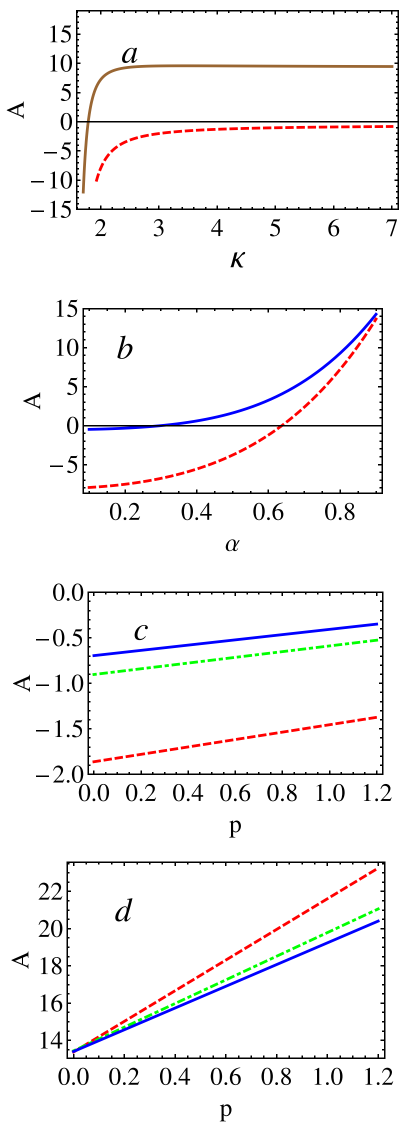

FIG. 3. Effect of superthermality, wave coupling parameter, and positrons on nonlinearity coefficient A. Plot (a): A versus κ for $p = 0.2$ and $\alpha = 0.1$ (dashed red curve), $\alpha = 0.8$ (solid brown curve). Plot (b): A versus α for $p = 0.2$ and $\kappa_e = \kappa_p = 2$ (dashed red curve), $\kappa_e = \kappa_p = \infty$ (Maxwellian limit, solid blue curve). Plot (c): A versus p for $\alpha = 0.2$ and $\kappa_e = \kappa_p = 3, 5, 7$ for the dashed (red), dotted–dashed (green), and solid (blue) curves, respectively. Plot (d): A versus p for $\alpha = 0.9$ and $\kappa_e = \kappa_p = 3, 5, 7$ for the dashed (red), dotted–dashed (green), and solid (blue) curves, respectively. The values of other parameters are $\sigma = 1$, $v_* = 0.3c_s$, and $u = 1.4v_*$.

VI. PARAMETRIC INVESTIGATION AND CONCLUSIONS

The theoretical results presented here are drawn for pulsar magnetosphere to let out the applicability of our analysis. It is believed that magnetic field can be as high as $B = 0.2G$ and number densities up to $n \sim 10^{14}\,\text{cm}^{-3}$ in the vicinity of pulsar magnetic poles having particle speed in the relativistic regimes,[52] the existence of protons around the atmosphere of pulsar magnetosphere is also possible.[22] It is important to mention that, although the electrons and positrons are relativistic,[52] the limit of nonrelativistic reasoning is still valid as the electrons and positrons can cool down into the nonrelativistic state due to the cyclotron emission. Therefore, the wave frequencies should be very less than the cyclotron one, which is the case for ion acoustic and drift waves.[53] The typical data for pulsar magnetosphere region is given by[22,52,53]

$$\text{n}_{i0} \sim 10^{14} — 10^{15}\,\text{cm}^{-3},$$

$$\text{n}_{e0} \sim 1.50 \times 10^{14} — 1.50 \times 10^{15}\,\text{cm}^{-3},$$

$$\text{n}_{p0} \sim 0.5 \times 10^{14} — 0.5 \times 10^{15}\,\text{cm}^{-3},$$

$$\text{T}_{e,p} = 10\,\text{eV}.$$

A. Pair annihilation time for electron positron ion plasma

In order to investigate the collective behavior of electron positron ion plasma, it is important to add discussion on the pair annihilation process for our plasma model: the electron positron has strong tendency to annihilate, producing gamma ray photons[52]

$$\text{e}^+ + \text{e}^- = \gamma + \gamma'.$$

To ignore the annihilation process, the electron positron plasma annihilation time, T_{ann} must be greater than the inverse of the characteristic frequencies of the plasma, which constitute (ω_{pj}), i.e.,

$$\omega_{pj} \ll \text{T}_{ann},$$

where ω_{pj} is the plasma frequency of the j-th species ($j = e, p, i$), the above inequality suggests that the time for plasma oscillations must be greater than annihilation process.

In order to investigate the collective modes in electron positron ion plasma, this annihilation time T_{ann} can be larger than 1 s for low density laboratory plasma; however, for higher densities and temperatures, one can calculate the annihilation time using the following procedure. In a nonrelativistic plasma, the expression for annihilation time takes the form[52]

$$\text{T}_{ann} = \frac{4}{3n_{\text{e,p0}}\sigma_t c}\left(\frac{E_{th}}{1 + 6E_{th}}\right),$$

where $n_{e,p0}$ represents the equilibrium electron/positron number densities, σ_t is the Thomson cross section of the electron, having numerical value equals to $6.65 \times 10^{-25}\,\text{cm}^2$. The symbol c stands for the speed of light and $E_{th}(=\frac{k_B T}{m_e c^2})$ is the normalized thermal energy, fulfilling the following threshold:[52]

$$\varrho \leq \mathrm{E}_{th} \leq 1.$$

Here, $\varrho (= 729 \times 10^{-3})$ represents the fine structure constant. For illustration, we have used the following numerical values to calculate the annihilation time for the nonrelativistic electron positron plasma:

$$\mathrm{n}_{e,p0} = 10^{14}\mathrm{cm}^{-3}, \mathrm{k}_B = 1.38 \times 10^{-16}\,\mathrm{ergs/deg(K)}, \\ \mathrm{c} = 3 \times 10^{10}\,\mathrm{cm/sec\ and\ m}_e = 9.1 \times 10^{-28}\,\mathrm{g}, \mathrm{T}_e = 10\,\mathrm{eV}.$$

Hence,

$$\omega_{pe}^{-1} = \left(\frac{4\pi n_{e,p0} e^2}{m_e}\right)^{-1/2} \sim (1653 \times 10^{-12}\,\mathrm{sec}),$$

$$\mathrm{T}_{ann} \sim (9126 \times 10^{-2}\,\mathrm{sec}),$$

$$\omega_{pe}^{-1} \ll \mathrm{T}_{ann}.$$

Here, we have shown the results numerically, it is evident from Figure 3(a) that, for a typical plasma parameters, the nonlinearity coefficient A invert sign against κ for higher value of α ($\approx$1), and hence, both compressive and rarefactive solitary waves can be obtained, while on the other hand, for small value of α (0.1), one can only obtain the rarefactive solitary waves in the present model. Similarly, in Figure 3(b), we have shown the behavior of nonlinear coefficient A versus wave coupling parameter (α) in superthermal plasma as well as in a Maxwellian plasma. One can see that for $\alpha < 0.6$, the nonlinear coefficient $A < 0$, and hence, one can have rarefactive solitons in a superthermal plasma having small value of kappa ($\kappa_e = \kappa_p = 2$), while for $\alpha > 0.6$, the coefficient of nonlinearity invert sign and support the hump like structures (compressive solitons) in the present model. It is important to mention here that for $\kappa_{e,p} \rightarrow \infty$ (Maxwellian limit), the solitons are sharper and taller, as evident from Figure 3(b). The effect of positrons on coefficient A has been demonstrated in Figures 3(c) and 3(d) with the effect of superthermality. It can be seen that increasing positron in the system makes the value of A to escalate and hence the amplitude suppresses. The role of wave coupling parameter α is also highlighted in Figures 3(c) and 3(d), one can see that for drift waves dominated solitons ($\alpha = 0.2$), the values of A are negatives, and hence, only rarefactive solitons are possible. It is important to point out that strong superthermality (low value of $\kappa_{e,p}$) makes the nonlinearity coefficient A to increase and more negative. On the other hand, for acoustic wave dominated solitons ($\alpha = 0.9$), the present model supports only compressive solitary waves, as the values A are positive and increasing with positrons. The parametric dependence of the amplitude and width of the solitary waves is well demonstrated in Figure 4. One can see that both compressive and rarefactive solitary waves can be obtained. The space coordinate η has been normalized with ρ_s which is of the order of 10^3 cm, the acoustic speed $c_s \sim 10^6$ cm/s, the ion gyrofrequency $\Omega_i \sim 10^4$ rad/s, and the soliton speed $u \sim 10^6$ cm/s, the parametric values shown are in agreement with space plasma environments.[22,52]

In the present work, we explored the dynamics of coupled ion acoustic and drift waves in a three-component electron positron ion plasma with the effect of

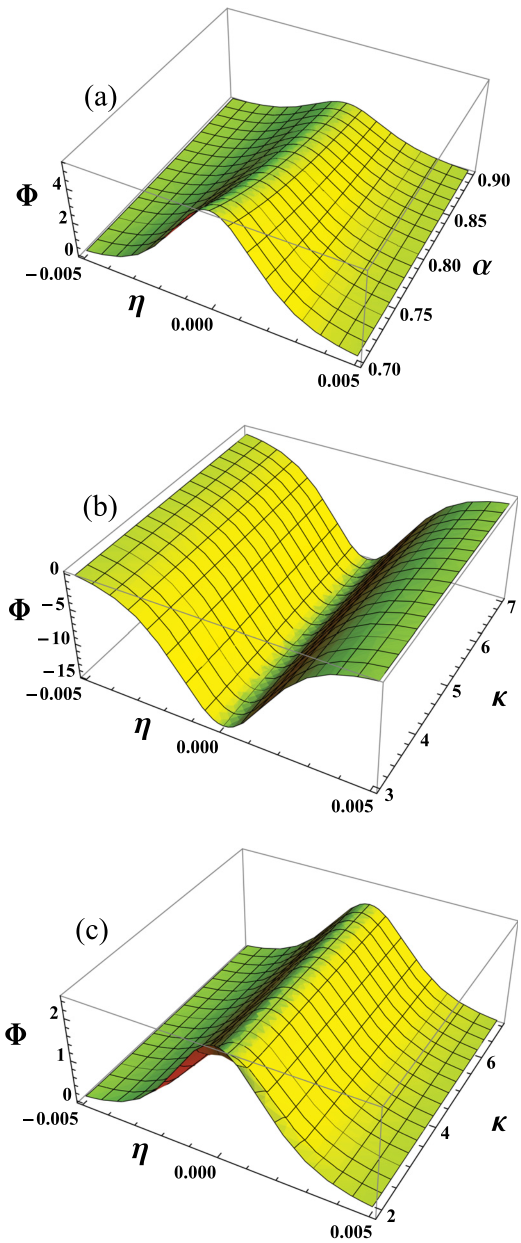

FIG. 4. Plot (a): Electrostatic potential Φ as a function of η and wave coupling parameter α for $\sigma = 1$, $\kappa_e = \kappa_p = 3$, $p = 0.2$, $B = 0.2G$, $v_* = 0.3c_s$, and $u = 1.4v_*$ Plot (b): Electrostatic potential Φ as a function of η and superthermality parameter κ for $\sigma = 1$, $\alpha = 0.1$, $p = 0.2$, $B = 0.2G$, $v_* = 0.3c_s$, and $u = 1.4v_*$. Plot (c): Electrostatic potential Φ as a function of η and superthermality parameter κ for $\sigma = 1$, $\alpha = 0.9$, $p = 0.2$, $B = 0.2G$, $v_* = 0.3c_s$, and $u = 1.4v_*$.

superthermality of electrons and positrons, which can exist in AGN and pulsars, in general, space plasma observation reveals solitons (pulses) of either positive or negative polarity. This actually depends on the plasma configuration (constituents, concentration, inertial versus, e.g., stationary species and so on). Similarly, drift waves exist universally in magnetized plasmas, producing the dominant mechanism for the transport of particles, energy, and momentum across magnetic field lines.[54] Here, we have found the following realities:

(1) In the linear limit, the phase velocity of ion acoustic and drift waves decreases with strong superthermality and

more positron content in the system via modifying the fundamental scales of plasma.

(2) In the nonlinear regime, first, coherent structures in the form of dipolar and monopolar vortices have been found. The role of superthermality and positrons has been highlighted. It is found that the speed of the nonlinear structures reduces with increase in the superthermality effect (low value of κ) and with the addition of more positrons in the system.

(3) Second, in case of scalar nonlinearity and weak dispersion, a Korteweg–de Vries-type equation is obtained, which support solitary wave solution. It is found that both compressive and rarefactive solitons are formed in the present model.

(4) We have shown our results for pulsar magnetospheric region in space plasma environment, which contains electron-positron-ion plasma.

ACKNOWLEDGMENTS

M.A. is thankful to Professor A. M. Mirza for having useful discussion on the topic. M.A. warmly acknowledges the Higher Education Commission (HEC), Islamabad, Pakistan, for the financial support via, (“Indigenous PhD 5000” and “IRSIP Fellowship” Programs). S.M. (CNPq-TWAS postdoctoral fellow-2014) acknowledges the support from CNPq, Brazilian National Council for Scientific and Technological Development—Brazil and TWAS, the academy of sciences for the developing world for the completion of this work.

[1] J. Weiland, *Collective Modes in Inhomogeneous Media: Kinetic and Advanced Fluid Theory* (IOP, Bristol, 2000).
[2] V. M. Vasyliunas, J. Geophys. Res. **73**, 2839–2884, doi:10.1029/JA073i009p02839 (1968).
[3] A. Hasegawa, K. Mima, and M. Duong-van, Phys. Rev. Lett. **54**, 2608–2610 (1985).
[4] V. Pierrard, J. Lemaire, and J. Lorentzian, J. Geophys. Res. **101**, 7923–7934, doi:10.1029/95JA03802 (1996).
[5] V. Pierrard, H. Lamy, and J. Lemaire, J. Geophys. Res. **109**, A02118, doi:10.1029/2003JA010069 (2004).
[6] M. A. Hellberg, R. L. Mace, R. J. Armstrong, and G. Karlstad, Phys. Plasmas **64**, 433–443 (2000).
[7] M. V. Goldman, D. L. Newman, and A. Mangeney, Phys. Rev. Lett. **99**, 145002 (2007).
[8] A. Olsson and P. Janhune, Ann. Geophys. **16**, 298–302 (1998).
[9] S. P. Christon, D. J. Williams, D. G. Mitchell, L. A. Frank, and Y. Huang, J. Geophys. Res. **94**, 13409–13424, doi:10.1029/JA094iA10p13409 (1989).
[10] M. P. Leubner and Z. Voros, J. Astrophys. **618**, 547–555 (2005).
[11] B. A. Shrauner and W. C. Feldman, J. Plasma Phys. **17**, 123–131 (1977).
[12] L. I. Rudakov and R. Z. Sagdeev, Sov. Phys. Dokl. **6**, 415 (1961).
[13] N. D Angelo and R. W. Motley, Phys. Fluids **6**, 422 (1963).
[14] W. Masood and A. M. Mirza, Astrophys. Space Sci. doi:10.1007/s10509-013-1759-9.
[15] A. M. Mirza, T. Farid, P. K. Shukla, and L. Stenflo, IEEE Trans. Plasma Sci. **29**, 298 (2001).
[16] Q. Haque, H. Saleem, and J. Vranjes, Phys. Plasmas **9**, 474 (2002).
[17] A. Mushtaq, R. Saeed, and Q. Haque, Phy. Plasmas **18**, 042305 (2011).
[18] W. Masood and A. Ahmad, Astrophys. Space Sci. **340**, 367–372 (2012).
[19] S. A. Shan and Q. Haque, Phys. Plasmas **19**, 084503 (2012).
[20] S. Mahmood, S. Kanwal, and Q. Haque, Phys. Plasmas **19**, 032306 (2012).
[21] S. I. Popel, S. V. Vladimirov, and P. K. Shukla, Phys. Plasmas **2**, 716 (1995).
[22] S. Mahmood, A. Mushtaq, and H. Saleem, New J. Phys. **5**, 28 (2003).
[23] H. P. Pakzad, Astrophys. Space Sci. **334**, 337 (2011).
[24] B. Sahu, Astrophys. Space Sci. **338**, 251 (2012).
[25] H. Alinejad, S. Sobhanian, and J. Mahmoodi, Phys. Plasmas **13**, 012304 (2006).
[26] E. I. El-Awady, S. A. El-Tantawy, W. M. Moslem, and P. K. Shukla, Phys. Lett. A **374**, 3216 (2010).
[27] F. C. Michel, Rev. Mod. Phys. **54**, 1 (1982).
[28] H. R. Miller and P. J. Witta, *Active Galactive Nuclei* (Springer, Berlin, 1987), p. 202.
[29] B. Kozlovsky, R. J. Murphy, and G. H. Share, Astrophys. J. **604**, 892 (2004).
[30] E. P. Liang, S. C. Wilks, and M. Tabak, Phys. Rev. Lett. **81**, 4887 (1998).
[31] C. M. Surko and T. J. Murphy, Phys. Fluids **2**, 1372 (1990).
[32] R. G. Greaves, M. D. Tinkle, and C. M. Surko, Phys. Plasmas **1**, 1439 (1994).
[33] M. Tinkle, R. G. Greaves, C. M. Surko, R. L. Spencer, and G. W. Mason, Phys. Rev. Lett. **72**, 352 (1994).
[34] R. G. Greaves and C. M. Surko, Phys. Rev. Lett. **75**, 3846 (1995).
[35] G. Gahn, G. D. Tsakiris, G. Pretzler, K. J. Witte, C. Delfin, C. G. Wahlstrom, and D. Habs, Appl. Phys. Lett. **77**, 2662 (2000).
[36] Y. B. Zel'dovich and I. D. Novikov, *Relativistic Astrophysics* (University of Chicago Press, Chicago, IL, 1981).
[37] S. L. Shapiro and S. A. Teakolsky, *Black Holes, White Dwarfs and Neutron Stars: The Physics of Compact Objects* (Wiley-Interscience, New York, 1983).
[38] G. Sarri, W. Schumaker, A. Di Piazza, M. Vargas, B. Dromey, M. E. Dieckmann, V. Chvykov, A. Maksimchuk, V. Yanovsky, Z. H. He, B. X. Hou, J. A. Nees, A. G. R. Thomas, C. H. Keitel, M. Zepf, and K. Krushelnick, Phys. Rev. Lett. **110**, 255002 (2013).
[39] H. Chen, M. Nakai, Y. Sentoku, Y. Arikawa, H. Azechi, S. Fujioka, C. Keane, S. Kojima, W. Goldstein, B. R. Maddox, N. Miyanaga, T. Morita, T. Nagai, H. Nishimura, T. Ozaki, J. Park, Y. Sakawa, H. Takabe, G. Williams, and Z. Zhang, New J. Phys. **15**, 065010 (2013).
[40] E. P. Liang, S. C. Wilks, and M. Tabak, Phys. Rev. Lett. **81**, 4887 (1998).
[41] H. Chen, S. C. Wilks, J. D. Bonlie, E. P. Liang, J. Myatt, D. F. Price, D. D. Meyerhofer, and P. Beiersdorfer, Phys. Rev. Lett. **102**, 105001 (2009).
[42] B. Shen and J. Meyer-ter-Vehn, J. Phys. Rev. E **65**, 016405 (2001).
[43] O. Adriani, G. C. Barbarino, and G. A. Bazilevskaya *et al.*, Nature **458**, 607 (2009).
[44] A. M. Galper, S. V. Koldashov, V. V. Mikhailov, and S. A. Voronov, Radiat. Meas. **26**, 375 (1996).
[45] S. A. Voronov, A. M. Galper, V. G. Kirilov-Ugryumov, S. V. Koldashov, and A. V. Popov, JETP Lett. **43**, 307 (1986).
[46] E. Fiandrini, J. Geophys. Res. **108**, 1402, doi:10.1029/2003JA009844 (2003).
[47] J. L. Hortwitz, D. L. Gallagher, and W. K. Peterson, *Geospace Mass and Energy Flow* (AGU, Washington, 1998), p. 343.
[48] F. Verheest, T. Cattaert, and M. Hellberg, Space Sci. Rev. **121**, 299 (2005).
[49] M. Tribeche, K. Aoutou, S. Younsi, and M. Amour, Phys. Plasmas **16**, 072103 (2009).
[50] E. F. El-Shamy, W. F. El-Taibany, E. K. El-Shewy, and K. H. El-Shorbagy, Astrophys. Space Sci. **338**, 279 (2012).
[51] Q. Haque and H. Saleem, Phys. Plasmas **10**, 3793 (2003).
[52] V. I. Karpman, C. A. Norman, D. Haar, and V. N. Tsytovich, Phys. Scr. **11**, 271 (1975).
[53] A. Esfandyari-Kalejahi, M. Mehdipoor, and M. Akbari-Moghanjoughi, Phys. Plasmas **16**, 052309 (2009).
[54] W. Horton, Rev. Mod. Phys. **71**, 735 (1999).